Self-Sorting in Supramolecular Assemblies

*Charlotte H. Chen[a], Liam C. Palmer[b, c, d], Samuel I. Stupp[a, b, c, d, e, f]**

[a]Department of Materials Science and Engineering, Northwestern University, 2220 Campus Drive, Evanston, IL 60208, USA.

[b]Simpson Querrey Institute, Northwestern University, 303 East Superior Street, Chicago, IL 60611, USA.

[c] Center for Bio-Inspired Energy Science, [d]Department of Chemistry, [e]Department of Biomedical Engineering, Northwestern University, 2145 Sheridan Road, Evanston, IL 60208, USA.

[f]Department of Medicine, Northwestern University, 676 North St. Clair Street, Chicago, Illinois 60611, USA

SI Appendix

S1: Peptide Synthesis

S2: Förster Resonance Energy Transfer (FRET)

S3: Confocal Microscopy of PA Mixtures

S4: Cryogenic Transmission Electron Microscopy (CryoTEM) of PA Mixtures

S5: Polarized Light Microscopy on PA Mixtures

S6: Small Angle X-Ray Scattering (SAXS)

S7: Fluorescence Recovery After Photobleaching (FRAP) on FITC and TAMRA PA

S8: Thioflavin T (ThT) Assay on Diluent PA

S9: Further Studies on FITC PA

S10: Modeling FRAP Data

S11: CryoTEM of FITC and TAMRA PA Alone

S12: Mechanical Perturbation of PA Matrix

S13: Introducing a Weak Hydrogen Bonding PA to the Diluent PA Matrix

S1: Peptide Synthesis

Previously reported synthesis methods[1] were used to prepare the peptide amphiphiles used here, including C_{16}-$V_3A_3E_3$ PA, C_{16}-$V_3A_3E_3$K-FITC (fluorescein isothiocyanate), C_{16}-$V_3A_3E_3$K-TAMRA (tetramethylrhodamine), C_{16}-$A_3G_3E_3$ PA, and C_{16}-$A_3G_3E_3$K-FITC.

Peptide amphiphiles molecules were synthesized using fluorenylmethyloxycarbonyl (Fmoc) solid phase peptide synthesis, by coupling Fmoc-protected amino acids (P3 BioSystems, Louisville, KY, USA) from Rink amide MBHA resin (Novabiochem [EMD Millipore], Billerica, MA, USA). All amino acid couplings were performed in a CEM Liberty microwave-assisted peptide synthesizer (CEM, Matthews, NC, USA), using default microwave settings. Fmoc groups were deprotected using 20% 4-methylpiperidine and 0.1 M hydroxybenzotriazole (HOBt) in dimethylformamide (DMF) at 75 °C for 3–4 min. Amino acids were coupled using 5 molar equivalents (equiv) of protected amino acid, 5 equiv *O*-benzotriazole-*N*, *N*, *N*′, *N*′-tetramethyluronium hexafluorophosphate (HBTU) and 10 equiv *N*,*N*-diisopropylethylamine (DIEA), at 75 °C for 5–10 min. Using this same procedure, palmitic acid (C_{16}) was conjugated to the N-terminus of the peptide. After each coupling, unreacted amines were capped using 0.5 M acetic anhydride, 0.125 M DIEA and 0.015 M HOBt in DMF, at 65 °C for 2 minutes.

Conjugation of fluorophores to PA: All fluorophores (FITC or TAMRA) were conjugated to the amine on a lysine side chain, which was Mtt-protected during the peptide synthesis procedure described above. For this purpose, Fmoc-Lys(Mtt)-OH (P3 BioSystems, Louisville, KY, USA) was used. To expose the amine on the side chain, Mtt was deprotected using 1% trifluoroacetic acid, 3% triisopropylsilane in dichloromethane (DCM), for 15 minutes. After Mtt deprotection, either 5(6)-carboxytetramethylrhodamine (TAMRA acid) or fluorescein isothiocyanate (FITC) were coupled. When coupling TAMRA, the reaction was conducted with 1.5 equiv TAMRA, 1.5 equiv benzotriazol-1-yl-oxytripyrrolidinophosphonium hexafluorophosphate (PyBOP), in DMF with 8-10 times molar excess of DIEA. When coupling FITC, the

same reaction conditions were used except there was no PyBOP. Fluorophore couplings for both dyes were conducted overnight.

Completed PA molecules were cleaved off the resin using a solution of 95:2.5:2.5 trifluoroacetic acid/triisopropylsilane/water for 2–3 h. Volatile solvents were removed with rotary evaporation, and the PA was precipitated with cold diethyl ether and dried using a fritted filter. The PA was then purified by preparatory scale reverse phase high-performance liquid chromatography (HPLC, Varian), using a Phenomenex Gemini column (C18 stationary phase, 5 µm, 100 Å pore size, either 30 × 150 mm or 50 x 250 mm). A mobile phase of acetonitrile and water was used, both containing 0.1% NH_4OH to aid solubility of acidic PA. Pure fractions were identified and collected, using electrospray ionization (ESI) mass spectroscopy. Excess acetonitrile was removed with rotary evaporation, freeze-dried, and the powders stored at -20°C until use. The purity of PA molecules was confirmed using liquid chromatography-mass spectroscopy (LC-MS), which was performed using an Agilent 6520 QTOF-LCMS with a similar Phenomenex column (Figures S1–S3).

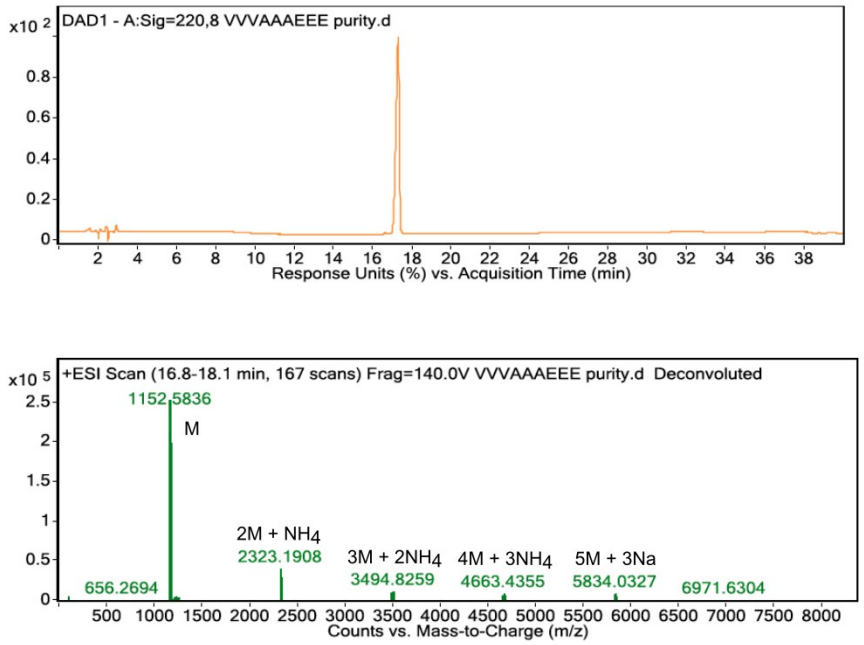

Figure S1. LC-MS analysis of $V_3A_3E_3$ PA (chemical structure shown in Figure 1 of the main text).

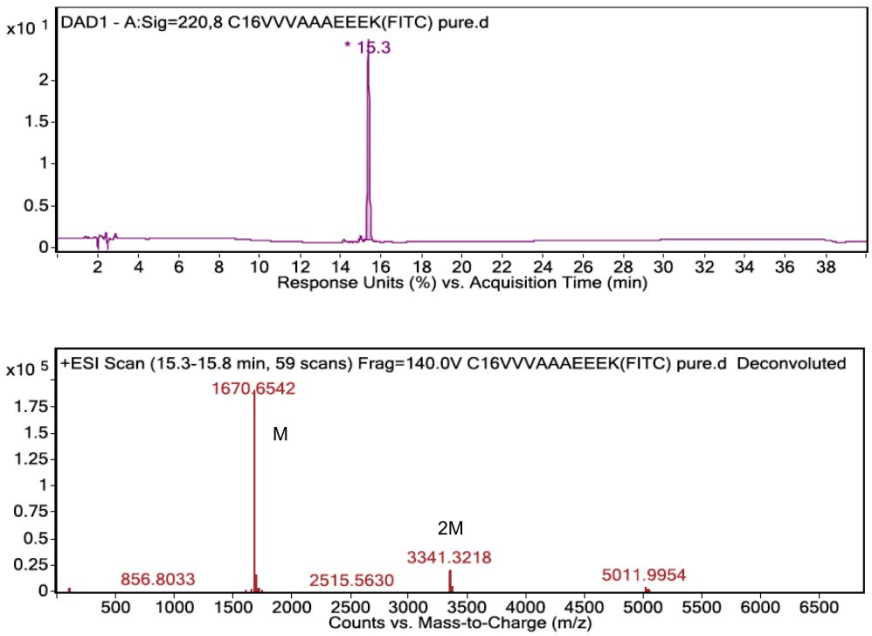

Figure S2. LC-MS analysis of $V_3A_3E_3K$-FITC PA (chemical structure shown in Figure 1 of the main text).

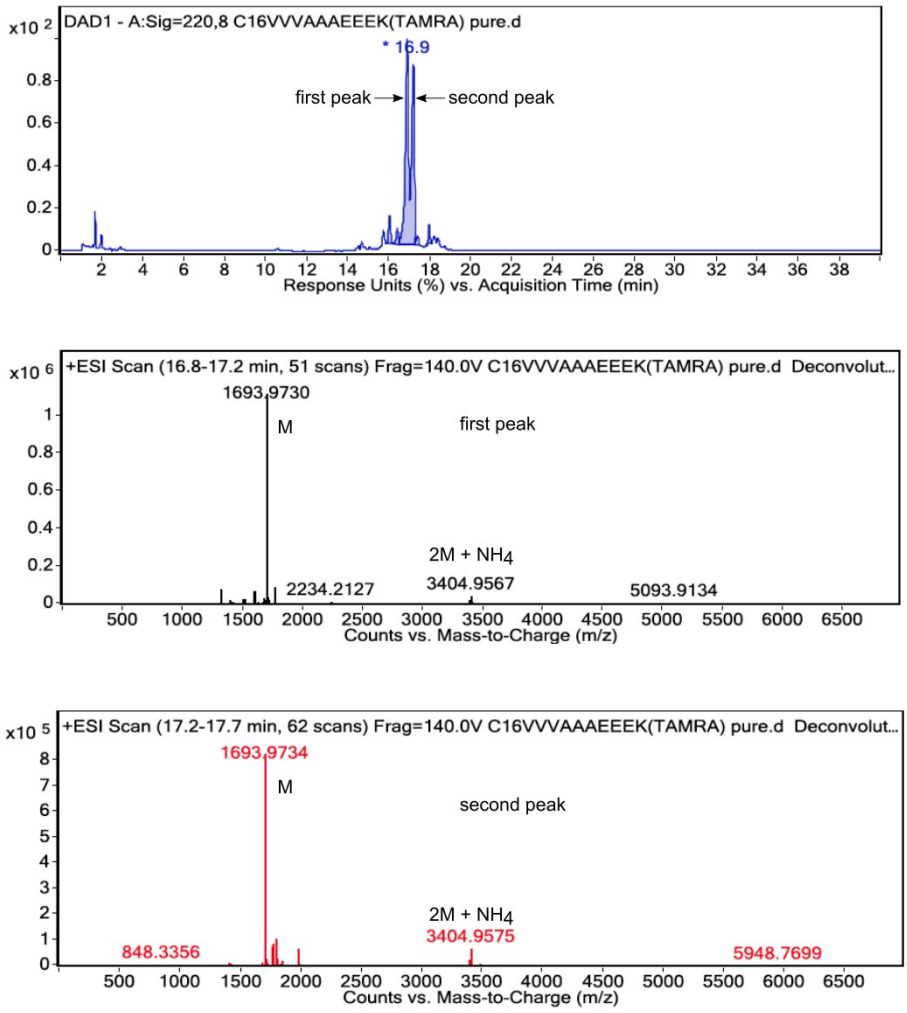

Figure S3. LC-MS analysis of $V_3A_3E_3K$-TAMRA PA (chemical structure shown in Figure 1 of the main text). The two peaks have the same mass and are different isomers of TAMRA. The PA is ~87% pure.

S2: FRET (Förster resonance energy transfer)

More detailed PA mixture preparation:

$V_3A_3E_3$ (diluent PA), $V_3A_3E_3K$-FITC (FITC PA), and $V_3A_3E_3K$-TAMRA (TAMRA PA) powders were all separately dissolved to 2 wt%. Diluent PA (at 2 wt%) was divided into two aliquots, and 1% (volume/volume) of 2 wt% $V_3A_3E_3K$-FITC PA was added to one aliquot, and 1% (volume/volume) of 2 wt% $V_3A_3E_3K$-TAMRA PA to the other aliquot. These PA solutions containing either FITC- or TAMRA-labeled PA were further split into aliquots, and diluted to 1 wt% PA with an equal volume of pure water or NaCl

solution. For example, PA solutions containing 26 mM NaCl were diluted from 2 to 1 wt% PA by adding equal volume 52 mM NaCl. Next, diluent + FITC PA solutions were mixed with diluent + TAMRA PA solutions containing the same NaCl concentration. These PA mixtures were either analyzed immediately (freshly dissolved samples), or after undergoing a heating and cooling cycle (80°C for 30 minutes followed by slow cooling overnight, annealed samples). When samples were annealed, they were subject to heating immediately after the initial mixing.

FRET spectral readings:

PA samples (50 μL) were loaded into a 96-well black plate with a clear bottom, which was analyzed using a Cytation^{TM}3 (BioTek, Winooski, VT, USA). The solutions were excited at 450 nm (direct FITC excitation), and fluorescence spectra collected from 480 – 700 nm, which covers both FITC and TAMRA emission. As a comparison, TAMRA was directly excited at 530 nm, and the emission spectra collected from 560 – 700 nm to observe rhodamine emission. Emission from direct rhodamine excitation for freshly dissolved and annealed $V_3A_3E_3$ PA mixtures are shown below.

Interestingly, in the freshly dissolved samples, there are no differences in emission from direct TAMRA excitation (Figure **S4**), while in the annealed samples, TAMRA emission intensity increases with NaCl concentration. The FRET spectra show little changes upon annealing in the 26 and 150 mM NaCl samples, and were also consistent with confocal micrographs (Figure 2a in main text). Intriguingly, this trend of TAMRA emission increasing as NaCl amount increases is directly opposite to the trend observed with FITC (Section S9 below).

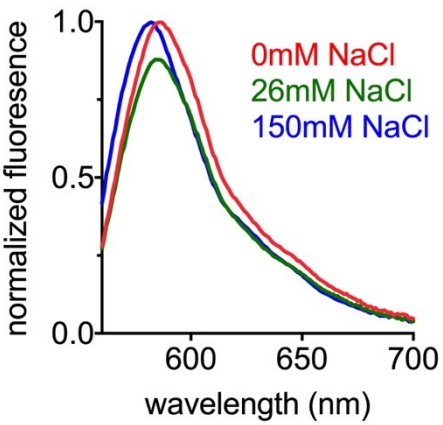

Figure S4: TAMRA emission from direct TAMRA excitation of freshly dissolved PA mixtures, containing the indicated salt concentrations. Excitation 530 nm.

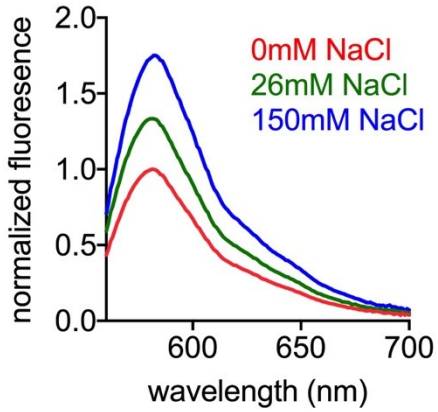

Figure S5: TAMRA emission from direct TAMRA excitation of annealed PA mixtures, containing the indicated salt concentrations. Excitation 530 nm.

***Note:** For the FRET experiments described above and shown in Figure 2 of the main text, the fluorescence spectra were all normalized to the highest fluorescent intensity detected in the 0 mM NaCl sample. The experiment was repeated four times, and the normalized fluorescence spectra were averaged together. Thus, the data in Figure 2a, S4, and S5 are the average of four experiments. In all other FRET experiments shown in the Supporting Information, the fluorescence spectra is one representative experiment.

FRET ratio calculations

The normalized FRET spectra for each sample, obtained as described above, were deconvoluted using Igor Pro 6.3 (WaveMetrics, Portland, Oregon, USA). An example of a deconvolution is shown below in Figure S6. The FRET ratio was then calculated as:

$$\frac{F_A}{F_A + F_D}$$

where F_A is the intensity of acceptor emission and F_D is the intensity of donor emission. Thus, in the example shown in Figure S6, we have:

$$\frac{F_A}{F_A + F_D} = \frac{0.40105}{0.40105 + 0.8325} = 0.325$$

Although this calculation is complicated by the self-quenching behavior of FITC (Section S9 below) and the overlap in emission spectra of FITC and TAMRA, the data still reveals trends between the samples.

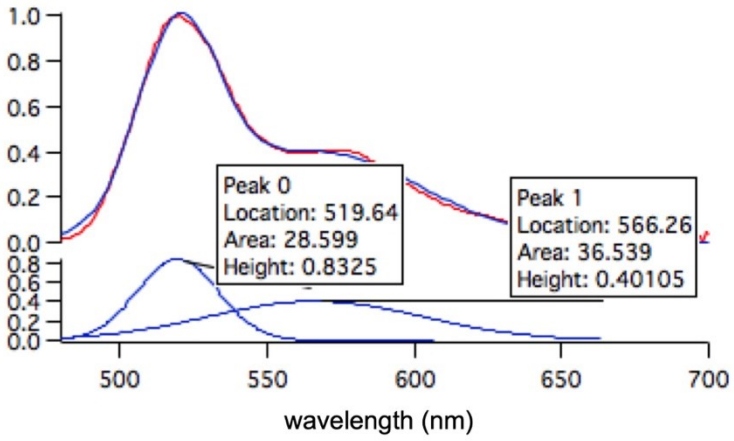

Figure S6: One example of a deconvolution to separate the FITC and TAMRA peaks in a FRET emission spectrum. The left peak is FITC emission and the right peak is TAMRA emission.

FRET experiment with variable heating times

We examined FRET behavior after various heating times, to determine if 30 minutes of heating and a slow cooling step were necessary to cause the changes shown in Figure 2b. A diluent, FITC, and TAMRA PA mixture containing 1 wt% PA and no NaCl was prepared as described above, and then heated at 80°C for the indicated times. Afterwards, the samples were immediately submerged in room temperature water after heating, so did not undergo the typical slow cooling step in the annealing procedure. All samples began heating at the same time, and samples with shorter heating times were stored at room temperature while other samples continued to heat. For example, the 10-minute sample was heated for 10 minutes and then stored at room temperature for 20 minutes while the 30-minute sample continued heating. The fresh, unheated sample was simply stored at room temperature for 30 minutes.

The data below shows that even with 5 minutes of heating, the FRET signal transitions to show less acceptor excitation and less donor quenching, and the spectra begins to look like that of annealed PA mixtures (Figure 2a in the main text). Simply aging the sample for 30 minutes does not cause the same effect.

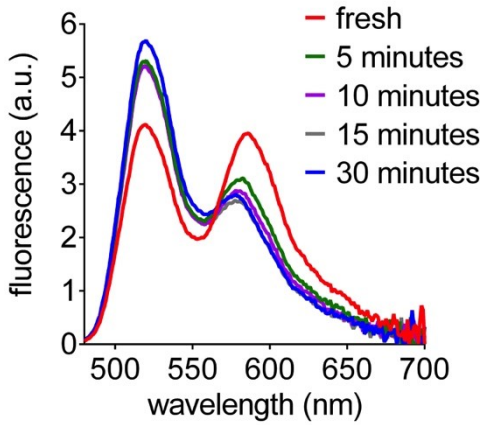

Figure S7: FRET spectra of PA mixtures containing 0 mM NaCl, heated at 80°C for the indicated times. Excitation 450 nm.

FRET experiment with varying PA concentration

Freshly dissolved diluent, FITC, and TAMRA PA mixtures, with 1 wt% PA and 0 mM NaCl, were prepared as described above. Through serial dilutions in pure water, freshly dissolved mixtures of 0.5, 0.25, 0.125, and 0.0625 wt% PA were prepared, which simultaneously reduces the concentration of diluent, FITC, and TAMRA PA in solution. These solutions were thermally annealed (80°C 30 minutes, slow cool overnight), and their FRET spectra collected as described above**.** TAMRA emission from direct excitation at 530 nm is also shown. As expected, the overall signal decreases as the concentration of fluorescent PA is decreased. However, the shape of the emission spectra never changes to suggest more FRET interactions between FITC and TAMRA PA.

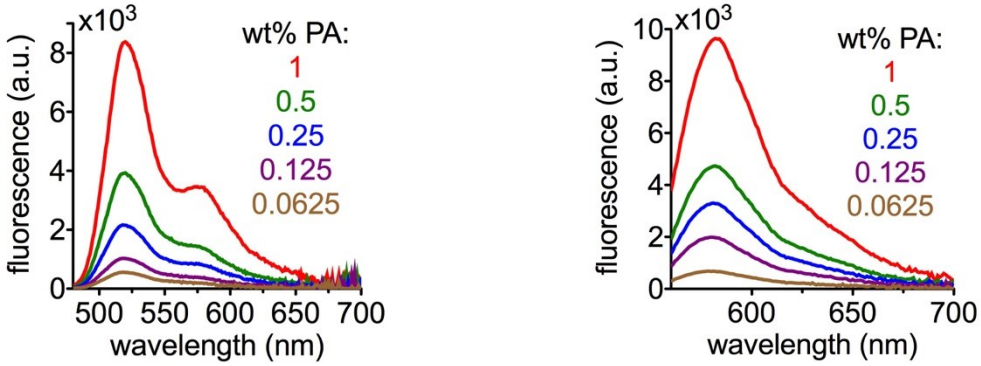

Figure S8. Left: FRET spectra of PA mixtures at indicated PA concentrations. Excitation: 450 nm. **Right:** TAMRA emission from direct excitation of the same samples shown on the left. Excitation: 530 nm.

FRET experiment varying when NaCl is added

Annealed diluent, FITC, and TAMRA PA mixtures, containing 1wt% PA and either 0 or 150 mM NaCl, were prepared as described above. All samples were then diluted to 0.5 wt% PA for this experiment in three different ways:

1.) 0 mM NaCl salt: PA annealed at 1 wt% in 0 mM NaCl, diluted to 0.5 wt% with pure water

2.) 75 mM NaCl salt (before): PA annealed at 1 wt% in 150 mM NaCl, diluted to 0.5 wt% with pure water
3.) 75 mM NaCl salt (after): PA annealed at 1 wt% in 0 mM NaCl, diluted to 0.5 wt% with 150 mM NaCl

Samples 2 and 3 above contain the same final PA and salt concentration (0.5 wt% PA, 75 mM NaCl), but the NaCl was added at different times during processing. Sample 1 serves as a control with no NaCl. FRET spectra on these solutions were collected as described above**.** TAMRA emission from direct excitation at 530 nm is also shown.

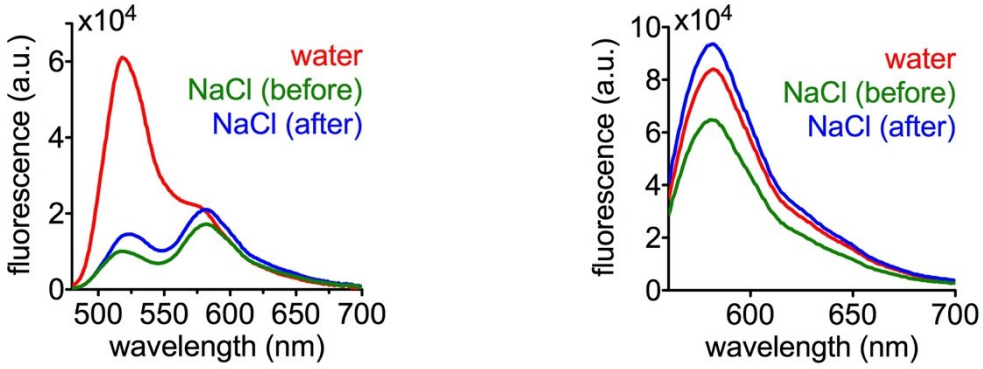

Figure S9: Left: FRET spectra of annealed PA mixtures containing no NaCl, or NaCl added either before or after annealing. Excitation: 450 nm. **Right:** TAMRA emission from direct excitation of the same samples shown on the left. Excitation: 530 nm.

S3: Confocal Microscopy of Diluent, FITC, and TAMRA PAs

Annealed PA mixtures containing diluent, FITC, and TAMRA PA were prepared as described in section **S2**, using the same exact procedure as for FRET experiments. PA solutions (50 μL) were pipetted onto a glass cover slip for imaging at 40x on a Nikon A1R microscope, using the 488 and 561 nm laser lines. Additional images of the samples in Figure 2c-e of the main text are shown below. These images show that while the PA solutions can exhibit a variety of micron-scale features, the 26 mM and 150 mM NaCl samples always tend to show more overlap between the two channels. We note that

the FRET data is a spectroscopic measurement of the entire solution (50 μL of solution is used for both FRET and confocal experiments), which would encompass all observed features in these solutions. In the 26 mM NaCl sample, a small portion was found to show some separation of the channels (indicated with an asterisk in Figure S11); however, FRET experiments on 26 mM NaCl samples consistently showed more fluorophore interaction than 0 mM NaCl samples (Figure 2b of main text).

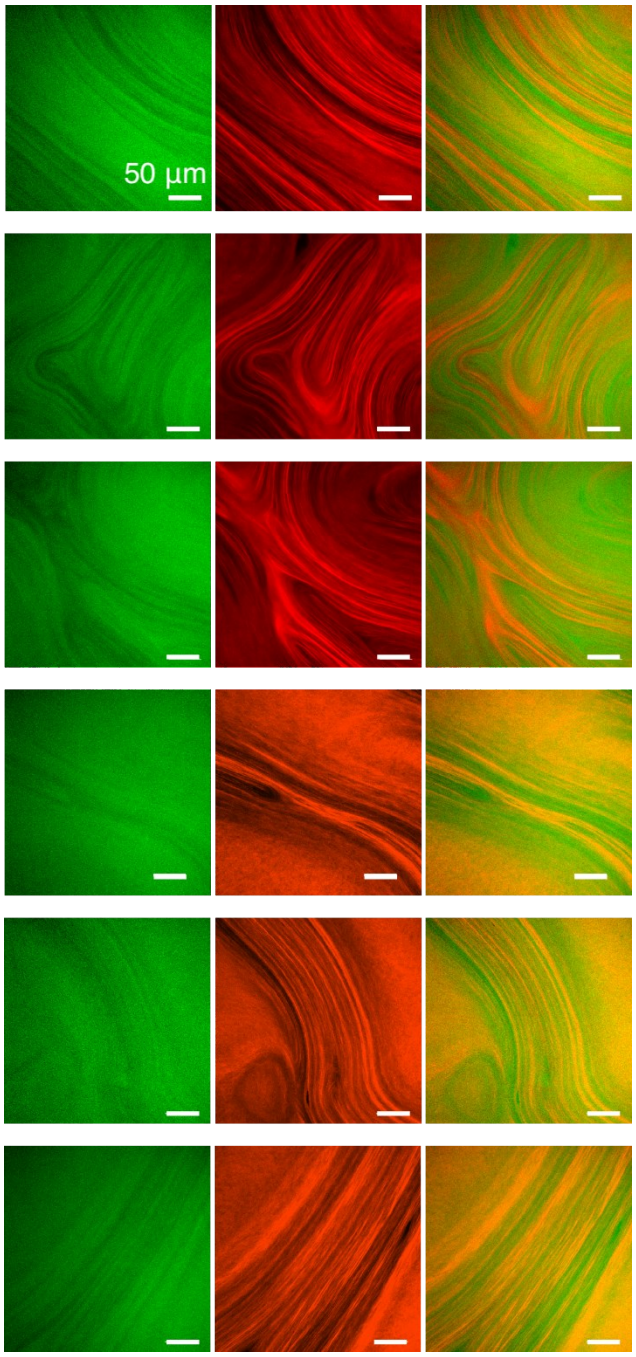

Figure S10: Additional confocal images of PA mixture with 0 mM NaCl, the sample shown in Figure 2c of the main text.

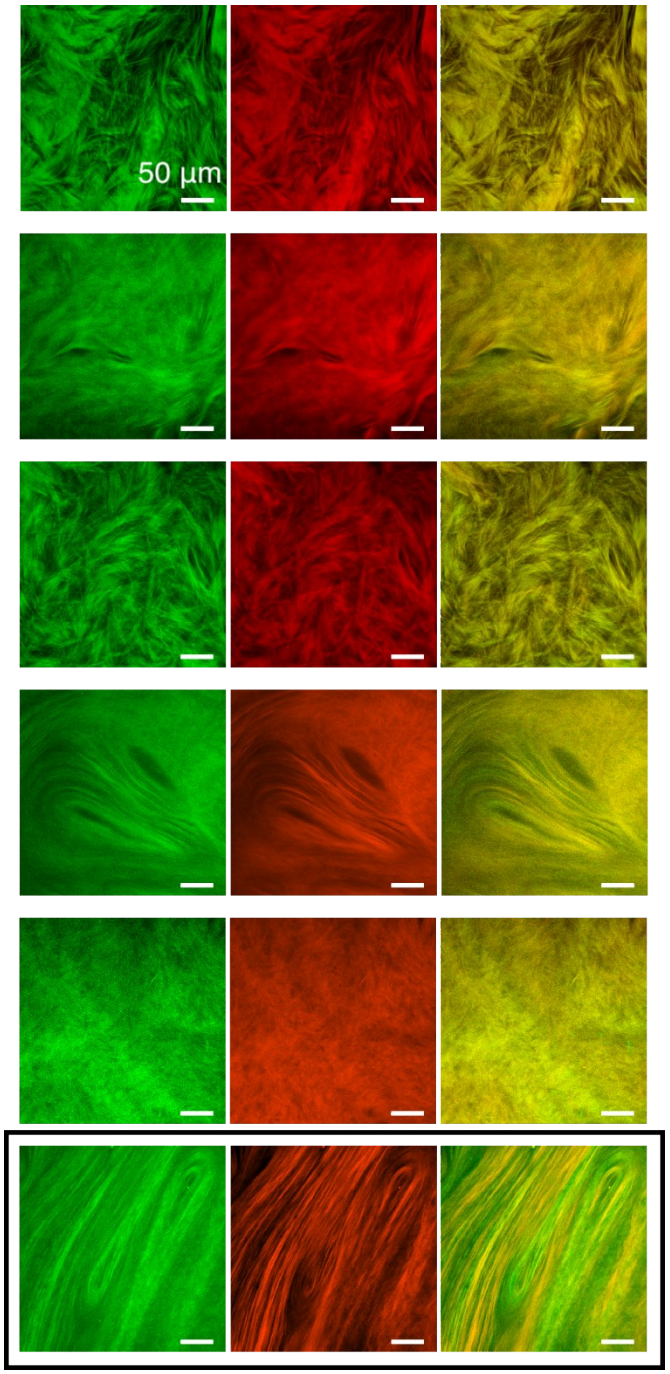

Figure S11: Additional confocal images of PA mixture with 26 mM NaCl, the sample shown in Figure 2d of the main text. The box represents a small portion of the sample that was unlike the majority.

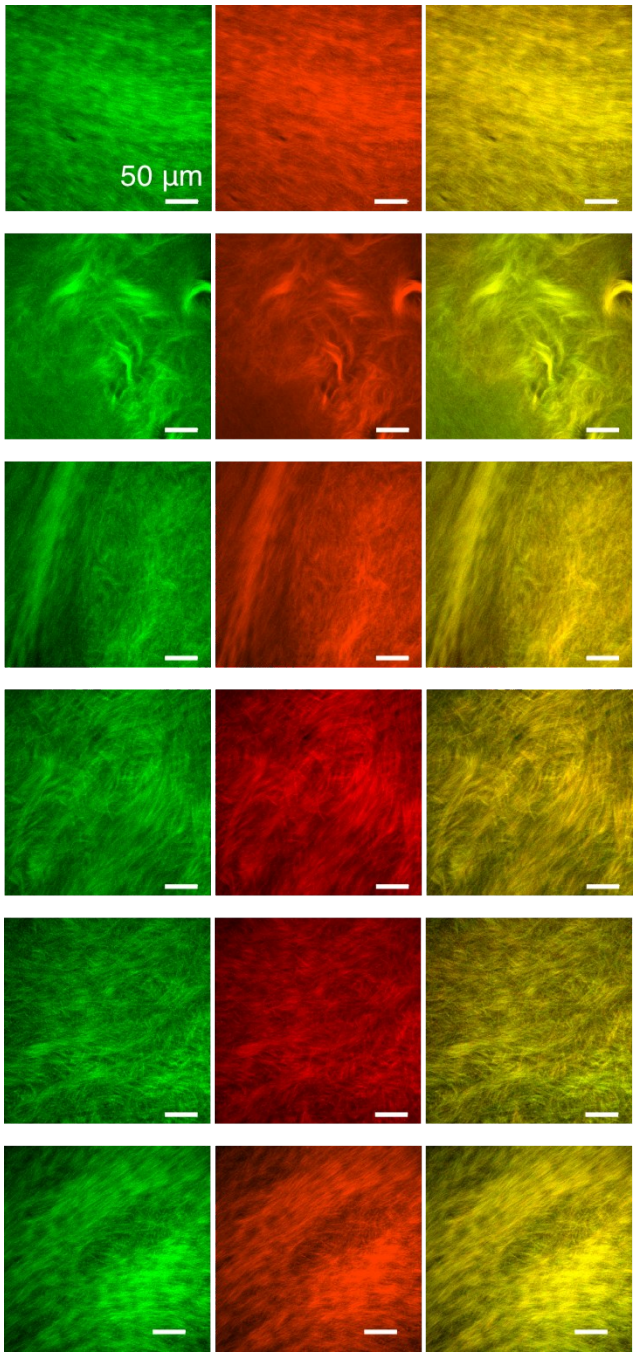

Figure S12: Additional confocal images of PA mixture with 150 mM NaCl, the sample shown in Figure 2e of the main text.

S4: Cryogenic Transmission Electron Microscopy (CryoTEM) of PA Mixtures

Annealed PA mixtures containing diluent, FITC, and TAMRA PA were prepared as described in section **S2**, using the same exact procedure as for FRET and confocal microscopy experiments. PA samples were diluted 1:100 in pure water immediately before blotting for imaging. These diluted samples (6.5 μL) were deposited onto 300-mesh copper grids with lacey carbon film (Electron Microscopy Sciences, Hatfield, PA, USA), inside a FEI Vitrobot Mark IV (FEI, Hillsboro, OR, USA), which was maintained around 95% humidity. Before use, the copper grids were glow discharged for 30 seconds in a PELCO easiGlow system (Ted Pella, Inc., Redding, CA, USA). The samples were plunged into liquid ethane, and then transferred to a Gatan 626 cryo-holder (Gatan, Pleasanton, CA, USA) while submerged in liquid nitrogen. Samples were imaged on a JEOL 1230 TEM operating at 100 kV, and micrographs were captured with a bottom-mounted Gatan 832 camera.

S5: Polarized Light Microscopy on PA Mixtures

Annealed PA mixtures containing diluent, FITC, and TAMRA PA were prepared as described in section **S2**, using the same exact procedure as for FRET and confocal microscopy experiments. PA solutions (50 μL) were pipetted onto a glass cover slide, and observed between cross-polarizers set to 90°.

S6: Small Angle X-Ray Scattering (SAXS)

Annealed PA mixtures containing diluent, FITC, and TAMRA PA were prepared as described in section **S2**, using the same exact procedure as for FRET and confocal microscopy experiments. SAXS measurements were taken at the Advanced Photon Source of Argonne National Laboratory, on Beamline 5-ID-D of the DuPont-Northwestern-Dow Collaborative Access Team (DND-CAT). A double crystal monochromator was used to select a beam energy of 17 keV (λ = 0.7293), and the detector was positioned 8.5 cm behind the sample. These samples were loaded into quartz capillaries, with 1.5 mm diameter with 0.1 mm wall thickness (Charles Supper,

Natick, MA, USA), and SAXS spectra were collected with an exposure time of 1 second. Two separate experiments were conducted.

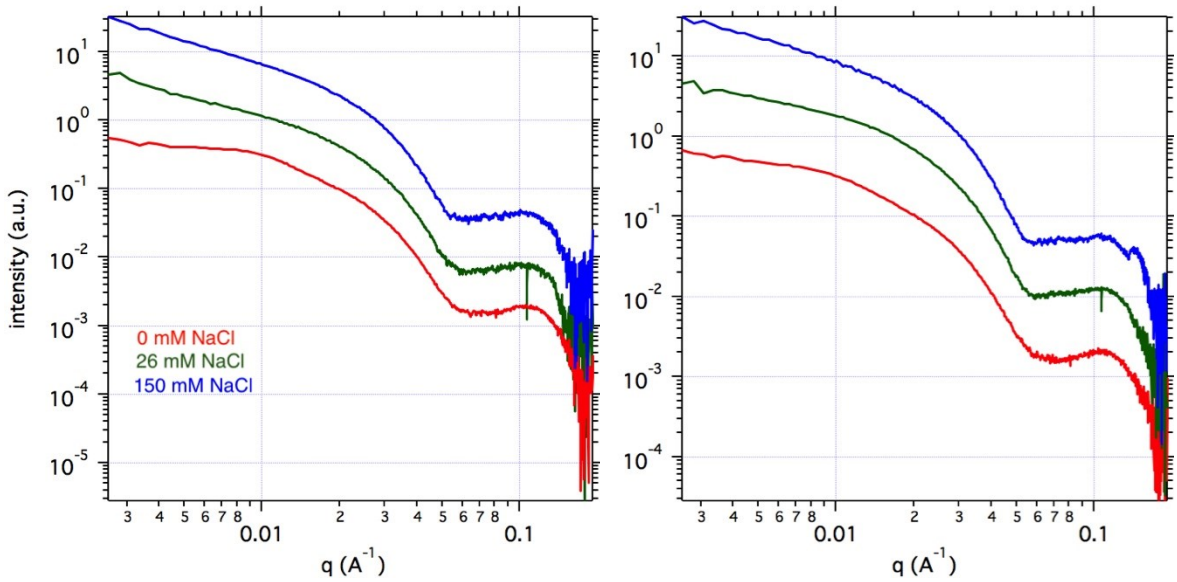

Figure S13: SAXS spectra of annealed PA mixtures with indicated NaCl amounts.

S7: Fluorescence Recovery After Photobleaching (FRAP) on FITC and TAMRA PA

More detailed PA preparation: For FITC PA experiments, $V_3A_3E_3$ PA and $V_3A_3E_3K$-FITC PA were first separately dissolved to 2 wt% with 30 mM NaOH. Next, 1% (volume/volume) of $V_3A_3E_3K$-FITC PA solution was added to the $V_3A_3E_3$ PA solution. This solution was then split into different aliquots, which were diluted to 1 wt% PA with equal volume pure water or NaCl solution to achieve the desired NaCl concentration. For example, PA samples containing 26 mM NaCl were diluted from 2 to 1 wt% PA by adding equal volume of 52 mM NaCl. This same procedure was also used to mix TAMRA PA samples.

PA sample imaging: PA solutions either analyzed immediately after they were created (freshly dissolved samples), or after they were subject to a heating and cooling cycle (80°C for 30 minutes, slow cool overnight). PA samples (50 μL) were pipetted onto a

glass cover slip for imaging. FITC PA was imaged with the 488 nm laser line while TAMRA PA was imaged with the 561 laser line, both using a 40x objective on a Leica SP5 confocal microscope (Leica, Wetzler, Germany).

FRAP procedure: After confocal imaging, the same PA samples were subject to photobleaching. For FITC PA samples, circles 10 μm in diameter were photobleached with the 488 nm laser line at 100% power. For TAMRA PA samples, squares that were 10 μm long on each side were photobleached instead. This is because, due to the high rate of photobleaching in TAMRA PA, the FRAP configuration does not allow photobleaching of circles. During photobleaching, the microscope zooms in on a square around the bleach spot, so if the bleach spot is a circle, the area outside the circle will be subject to the lower laser intensity used for imaging as opposed to the higher laser intensity used for photobleaching. In the case of TAMRA PA, this exposure to lower laser intensity causes the area outside the circle to become noticeably lower than the unbleached PA outside the zoom box. However, this area still had a higher fluorescence intensity than the area within the actual bleach circle. To avoid this problem, the entire square was photobleached. FITC PA appears to be less susceptible to photobleaching than TAMRA PA, so circles could be bleached. For both experiments, the microscope scanned a 512 x 512 pixel area at 1000 Hz, allowing an image to be captured approximately every 0.263 seconds. Fluorescence intensity in the photobleached area was normalized to fluorescence intensity in an image area that was not photobleached, in order to account for photobleaching due to imaging. The following equation was used to obtain the final reported values ($I_{corrected}$):

$$I_{corrected} = I_{measured} * \frac{I_{unbleached}^{0}}{I_{unbleached}}$$

where the initial unbleached value ($I_{unbleached}^{0}$) is the average of 5 pre-bleach frames, in the unbleached image area. These corrected intensities ($I_{corrected}$) were then used to obtain a value between 0 and 1 ($I_{normalized}$, where 0 represents no recovery and 1 represents full recovery), and these values were plotted over time. The pre-bleach fluorescence

($I_{prebleach}$) was obtained by averaging the bleach spots fluorescence intensity in the 5 pre-bleach frames, while the post-bleach intensity ($I_{postbleach}$) was obtained by taking the bleach spot's fluorescence intensity immediately after photobleaching. The following equation was used to normalize fluorescence intensity in the bleach spot for all other time points:

$$I_{normalized} = \frac{I_{corrected} - I_{postbleach}}{I_{prebleach} - I_{postbleach}}$$

S8: Thioflavin T (ThT) Assay on Diluent PA

Since NaCl appears to affect FITC and TAMRA PA differently, we wanted to probe the effect of NaCl on diluent PA without fluorescent PAs. We probed the β-sheet content of the PA nanofibers with a ThT (Thioflavin T) assay. In a well-established technique, ThT dye is used to visualize amyloid fibrils, because its fluorescence is enhanced within the β-sheet-rich region of amyloid fibrils.[2] Our laboratory previously adapted this technique to probe the β-sheet content of PA nanofibers, and found that ThT fluorescence was decreased when the PA's ability for β-sheet formation was disrupted by molecular design.[3]

Diluent PA was first dissolved to 2 wt%, and then split into separate aliquots. These aliquots were then diluted to 1 wt% with equal volume of pure water or NaCl, such at the final PA solution contained 1 wt% PA and either 0, 26, or 150 mM NaCl. These solutions were analyzed while freshly dissolved. It was not possible to use this assay to analyze annealed PA samples, because the bundles created by the long nanofibers interfere with ThT dye diffusion. The 1 wt% PA samples were then mixed with a solution of ThT dye dissolved in pure water, such that the final concentrations of PA and ThT dye were 500 μM and 50 μM, respectively. This PA/ThT dye solution (100 μL) was loaded into a 96-well black plate with a clear bottom. The NaCl concentrations on the graph refer to the concentration of NaCl in the original 1 wt% PA solution, and not after

dilution for the ThT assay. The plate was read on a Cytation^{TM}3 (BioTek, Winooski, VT, USA), with excitation at 440 nm and emission spectra collected from 470 – 600 nm.

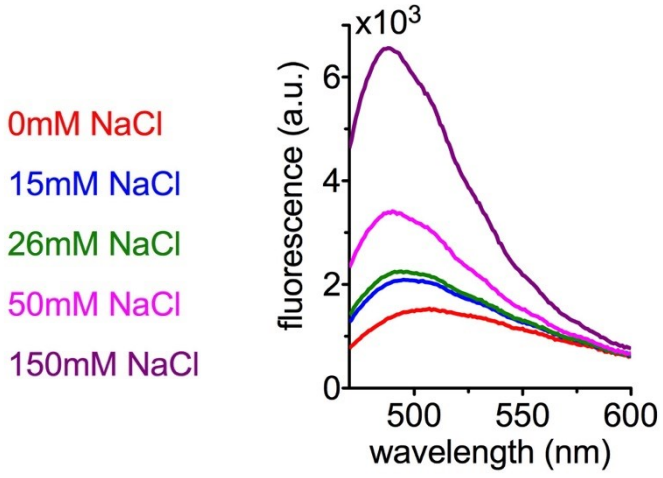

Figure S14. ThT fluorescence spectra when ThT is mixed with freshly dissolved PA, at indicated NaCl concentrations.

S9: Further Studies on FITC PA

In addition to those reported in the main text, several experiments show the sensitivity of FITC PA to NaCl concentration in the solvent.

Additional confocal micrographs

Diluent + FITC PA solutions were prepared as described in Section **S7**, and contained 1 wt% PA and 0, 15, 26, 50, 150, or 500 mM NaCl. These samples were thermally annealed, and then imaged with confocal microscopy as described in Section **S7**. After imaging, the same samples were photobleached for FRAP experiments. For comparison, we induced gelation of annealed PA solution containing no NaCl with 30 mM $CaCl_2$ (divalent vs. monovalent counterion). This instantly forms a physical gel.

Interestingly, the $CaCl_2$ gel has similar micron-scale features to PA *solutions* containing 15 – 26 mM NaCl. The 500 mM NaCl sample, which transitions from a solution to a gel upon annealing, shows highly distinct features from the other samples.

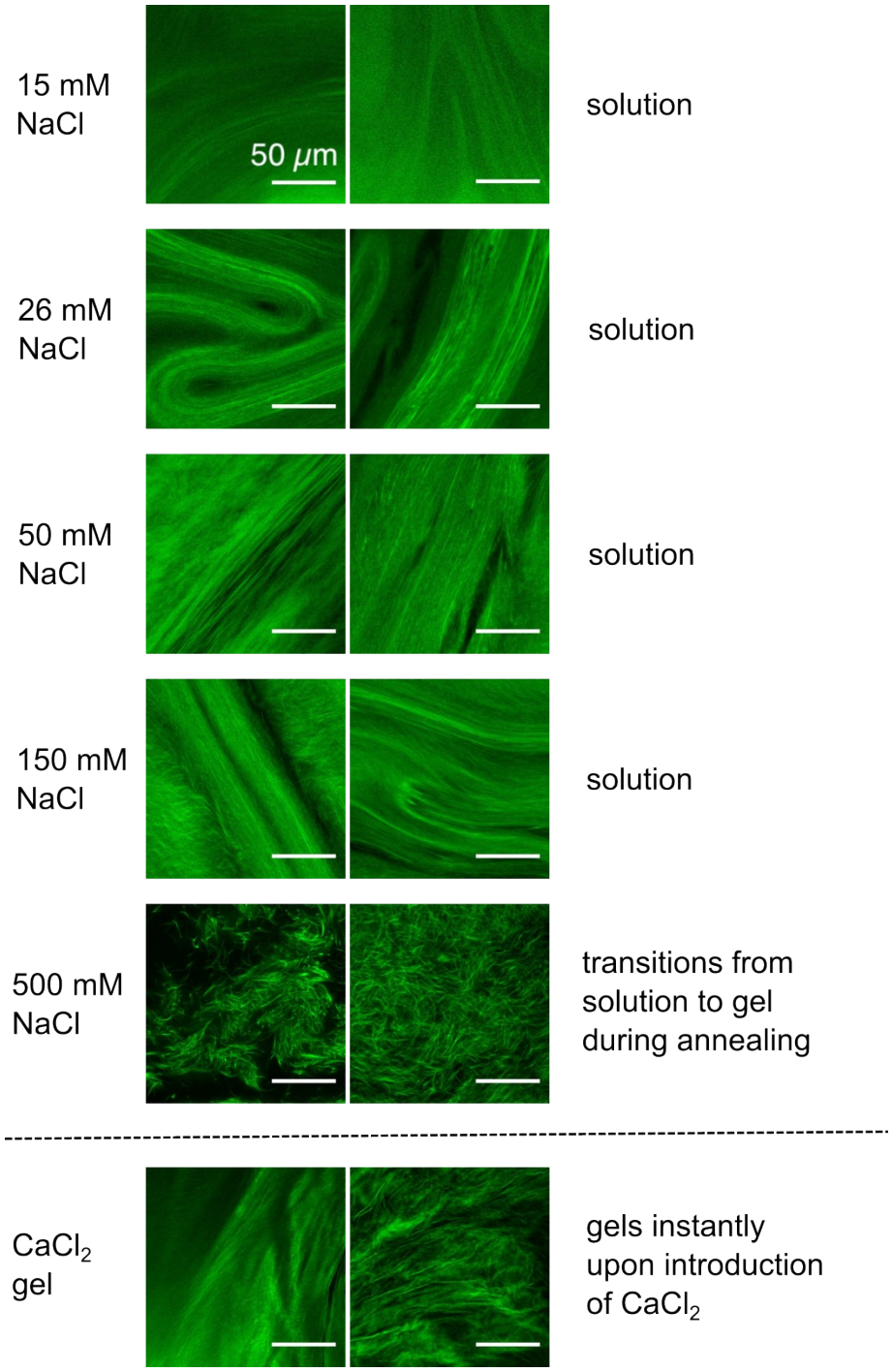

Figure S15. Confocal micrographs of annealed diluent + FITC PA samples, at indicated NaCl concentrations.

Additional FRAP samples and FRAP with free fluorescein dye:

We conducted the FRAP experiments reported in the main text (Figure 3-4 in main text, Section **S7)** at additional salt concentrations for FITC PA. The data shows a concentration-dependent effect of NaCl on FITC PA diffusion from 0 – 50 mM NaCl, with everything becoming immobile at higher concentrations (Figure S16). As expected, FITC PA in a $CaCl_2$ crosslinked, physical gel was completely immobile.

As a control, we repeated the FRAP experiments (Section **S7**) where fluorescein dye was not conjugated to PA, but was instead mixed with the PA solution. A 6 mg/mL solution of fluorescein sodium salt (Sigma Aldrich, St. Louis, MO, USA), dissolved in pure water, was mixed a 1 wt% annealed PA solution at 1% (volume/volume), for a final concentration of 30 μg/mL fluorescein sodium salt in the PA solution. These FRAP experiments showed that the salt-dependent trend observed with FITC-labeled PA does not occur with free fluorescein dye (Figure S16).

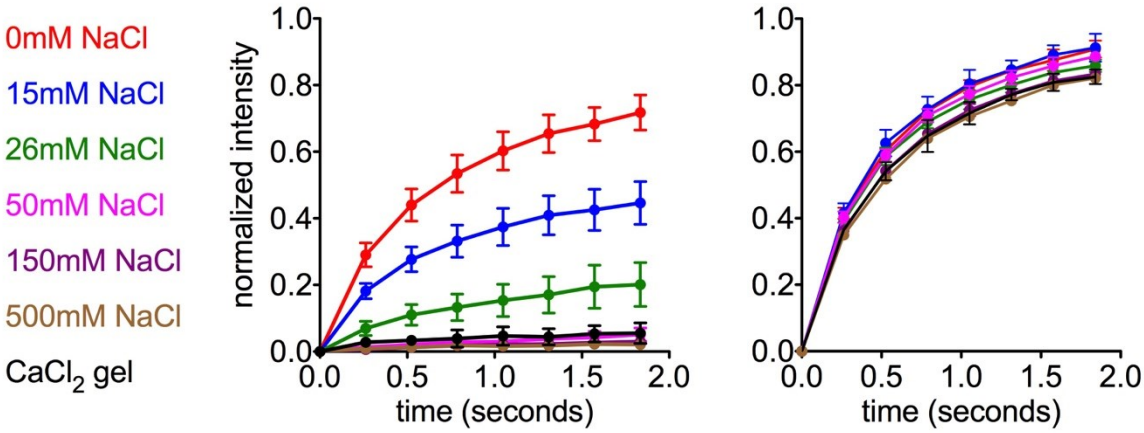

Figure S16. Left: Fluorescence recovery after photobleaching experiments on FITC PA mixed with diluent PA, at indicated NaCl concentrations. **Right:** Fluorescence recovery after photobleaching experiments on free fluorescein dye mixed with diluent PA, at indicated NaCl concentrations. The color key and y-axis label on the left also apply to the graph on the right.

Fluorescence Intensity of FITC PA Before and After Annealing

Diluent + FITC PA solutions were prepared as described in Section **S7**, and contained 1 wt% PA and 0 – 150 mM NaCl. They were analyzed either immediately (freshly dissolved) or after thermal annealing (80°C for 30 minutes, slow cool overnight). PA solutions (50 μL) were loaded into a 96-well black plate with a clear bottom. The plate was read on a Cytation^{TM}3 (BioTek, Winooski, VT, USA), with excitation at 450 nm and emission spectra collected from 480 – 700 nm.

Figure S17 shows that, in both freshly dissolved and annealed PA, NaCl induces fluorescence quenching of FITC PA mixed with diluent PA. Fluorescein is known to self-quench when two molecules come within a few nanometers of each other,[4] and our laboratory previously showed that salt counterions strengthen cohesion within the nanofiber by allowing charged PA molecules to pack closer together.[5] Thus, we hypothesize that the quenching is due to PA molecules packing more closely within the nanofiber, which allows for more self-quenching events. Interestingly, low salt concentrations (4–8 mM) cause fluorescein quenching freshly dissolved PA, but this effect seems to disappear when the PA is annealed.

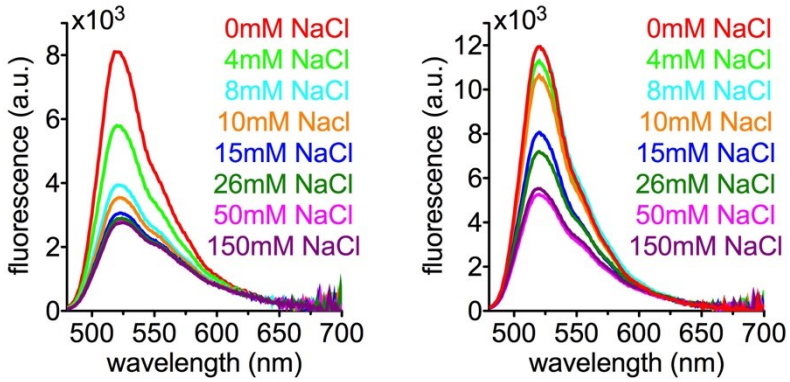

Figure S17. Fluorescence spectra FITC PA in freshly dissolved (left) and annealed (right) samples, in indicated amounts of NaCl.

We repeated the above experiments with free fluorescein dye as opposed to FITC PA, by preparing samples as described above, in the "*Additional FRAP samples and FRAP with free fluorescein dye"* section. Figure S18 shows that the same quenching effect is not observed.

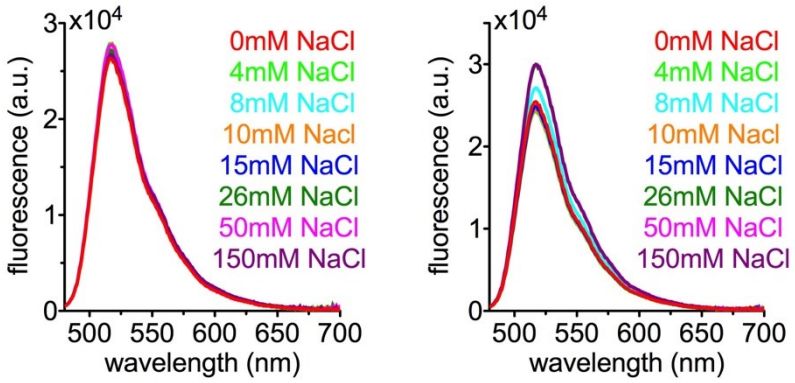

Figure S18. Fluorescence spectra free fluorescein dye in freshly dissolved (left) and annealed (right) samples, in indicated amounts of NaCl.

Fluorescence Intensity of FITC PA at 80°C

We studied the system *during* the thermal annealing procedure, when the solutions are held at 80°C for 30 minutes. Since it is not possible to conduct confocal microscopy or FRAP experiments at 80°C, we tracked the fluorescence intensity of FITC PA.

Freshly dissolved diluent + FITC PA samples were prepared as described in section **S7**, and control samples with free fluorescein dye were prepared as described above. Samples (50 μL) were loaded into a 96-well PCR plate, sealed, and placed into a CFX96 Touch™ Real-Time PCR Detection System (Bio-Rad Laboratories, Des Plaines, IL, USA). The temperature was set to and held at 80°C for 30 minutes (temperature and heating time for annealing PA solutions), and the fluorescence intensity of the PA solutions monitored every minute for the 30-minute duration.

For the entire 30 minutes of heating at 80°C, the signal of FITC PA was quenched in the presence of 26 or 150 mM NaCl (Figure S19) suggesting that the effects of salt on FITC PA (and possibly also diluent PA) persist even at elevated temperatures. Conversely, when free fluorescein dye is simply mixed with diluent PA, the presence of salt does not cause fluorescence quenching (Figure S19).

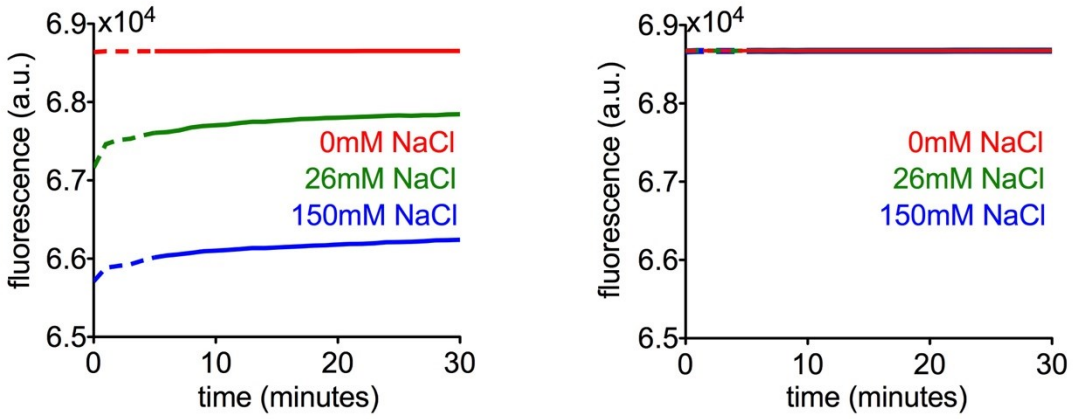

Figure S19. Fluorescence intensity of PA solutions held at 80°C for 30 minutes, in indicated amounts of NaCl, containing free fluorescein dye and no FITC PA. The dashed lines indicate an equilibration period where results may vary, before settling into the trend seen in the solid line portions.

Viscosity of Diluent + FITC PA Solutions

Since the effects of NaCl on FITC PA appear to persist at elevated temperatures, we wanted to further probe the effect of NaCl *after* annealing. We measured the viscosity of annealed diluent + FITC PA mixtures. Annealed diluent + FITC PA samples were prepared as described in section **S7,** and 200 μL of the sample was loaded onto the measuring plate (set to 23°C) of a MCR 302 rheometer (Anton Paar, Graz, Austria). Measurements were performed with the CP25-2 fixture (25 mm diameter cone-plate), which increased the shear rate from 1–100 s^{-1} over 240 seconds, and measured the

respondent shear stress. The final viscosity at 100 s^{-1} is reported, and the entire flow curves are also shown (Figure S20).

The viscosity measurements showed that PA samples containing no salt were more viscous than PA samples with NaCl (Figure S20). Since viscosity is a bulk measurement of the entire sample, it is not clear if the effects of salt are due to diluent PA or FITC PA. However, it is interesting that NaCl makes the samples less viscous, even though it causes diluent PA to show stronger hydrogen bonding (Figure S14) and FITC PA to pack closer together and become less mobile (Figure S15-19). This would suggest that PA assembles are more cohesive when salt is present, which is consistent with previous work,[5] so this result is slightly counterintuitive. We hypothesize that when NaCl allows the formation of more cohesive nanofibers, they may become more susceptible to breaking under shear.

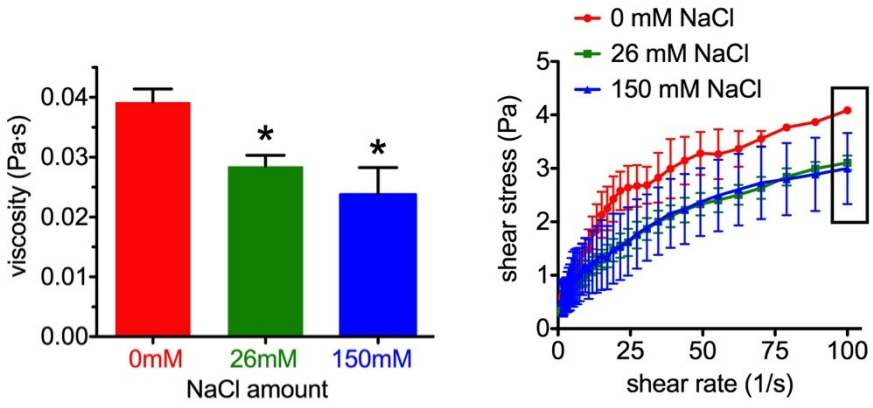

Figure S20. **Left:** Viscosity of diluent + FITC PA samples with indicated NaCl concentrations. **Right:** Full flow curves of diluent + FITC PA samples, the square indicates the data point used to calculate the viscosity reported in the left graph.

S10: Modeling FRAP Data

We modeled individual FRAP curves (averaged together in Figure 3g-h and Figure 4g-h of the main text) to describe the diffusion of fluorescent PA using a single exponential:

$$y = y_0(1 - e^{-t/\tau}) \qquad (1)$$

as described in the main text. This is a general equation of the form:

$$y = y_0 - Ae^{-\frac{(t - t_0)}{\tau}} \qquad (2)$$

where $y_0 = A$ and $t_0 = 0$. The experimental data (y versus t) was fitted to equation 2 using the **exp_XOffset** function in Igor Pro 6.3 (WaveMetrics, Portland, OR, USA). In this fitting, t_0 is automatically set to the first data point in the inputted curve, which was always 0 seconds in our FRAP data. In collecting our FRAP data, the first frame after photobleaching ($I_{postbleach}$) was always taken to be $t = 0\ seconds$, where the normalized intensity was set to 0 for 0 recovery. Since our FRAP data only has 8 data points and will therefore not be exactly precise, we did not force $y_0 = A$ in the curve fittings. However, we note that the values for y_0 and A were similar by visual inspection. From these fittings, we obtained the parameters y_0, τ, and A, and the parameter A was not used in further analysis. From τ, the half recovery time ($t_{1/2}$) of the mobile species can be calculated:

$$t_{1/2} = \tau\, ln(2) \qquad (3)$$

From this and the parameters of the FRAP experiment, the diffusion coefficient (D) of the mobile species can be calculated using the Soumpasis approximation[6]:

$$D = 0.224 \frac{w^2}{t_{1/2}} \qquad (4)$$

where w is the radius of the bleach area (5 μm). Using the Stokes–Einstein equation, we calculated hypothetical diffusion coefficient for 10 nm PA micelles and 200 nm PA short nanofibers, by setting ($R = 5\ nm, 100\ nm$):

$$D = \frac{k_B T}{6\pi\eta R} \qquad (5)$$

where k_B is Boltzmann's constant, T is temperature, and η is the viscosity of the solution. We used the viscosity of water for η, because the PA is dissolved in water and constitutes 1 wt% of the entire solution. Since the Stokes-Einstein equation assumes spherical objects diffusing through a uniform liquid medium, the size calculations will not accurately reflect anisotropic nanofibers or objects that are diffusing around long PA nanofibers, but we performed this calculation to estimate the size to an order of magnitude.

Since the collected FRAP data has only 8 data points due to constraints with imaging speed, and there are errors associated with fluorescence measurements, the curve fitting sometimes gave grossly and obviously inaccurate results. These fittings were excluded from our analysis. This was more prone to happen in samples with a large immobile fraction, because the amount of fluorescence recovery was small in these cases, so the assumed exponential behavior may not be detected. If the fitted parameters had an error several orders of magnitude greater than the fitted value, the fitting was excluded from our analysis. Also, the fitted parameter y_0 must be a value between 0 and 1 if it is to

represent normalized fluorescence, so fittings where y_0 was significantly larger than 1 were excluded from our analysis. Indeed, some of these excluded fittings may have described the absence of diffusion, where the mobile phase $y_0 \to 0$ and characteristic diffusion time $\tau \to \infty$. However, we did not want to arbitrarily exclude some fittings while including others as having a 100% immobile fraction, so we simply excluded these fittings. Furthermore, we did observe some degree of fluorescence recovery at $t \cong 1.8\ seconds$ in all samples, so we assumed that all samples had some amount of mobile fraction. We note that in one case, the mobile fraction was calculated to be almost exactly 1, which appeared to be an incorrect fitting. This data point was later excluded due to the removal of outliers (described below).

Of the data points that were not excluded due to an obviously incorrect fitting (described above), we systematically removed outliers. Because our FRAP data contains only 8 data points and therefore limited precision, we assumed that outliers in curve fitting parameters (y_0 and τ) were due to inaccuracies in the fitting as opposed to actual variations in the system's behavior. To identify and remove outliers, we employed the ROUT method,[7] which combines Robust regression and Outlier Removal, using GraphPad Prism 8 (GraphPad Software, San Diego, CA, USA). We chose Q = 10% for the ROUT analysis, which is relatively aggressive in detecting outliers, and relatively more likely to detect false outliers. We chose this parameter due to our assumption that most variation in the data was caused by lack of precision in the model, as opposed to variation in the actual system. Since y_0 and τ come from the same fitted equation, if one was excluded for a specific curve, the other parameter for that curve was automatically excluded too.

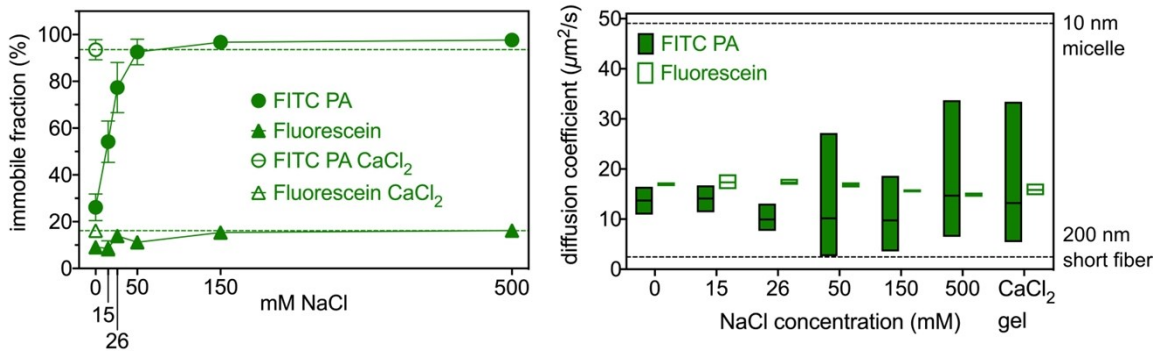

Figure S21. Modeling FITC PA FRAP data at additional NaCl concentrations. **Left**: Immobile fraction of FITC PA or fluorescein dye when mixed with diluent PA, at indicated conditions. The immobile fraction was calculated by modeling the FRAP data using a single exponential. The error bars represent the standard deviation. **Right**: Diffusion coefficient of mobile FITC PA or fluorescein dye, at indicated conditions. The half recovery time of the mobile fraction was extracted from a single exponential model of the FRAP data, and related to the diffusion coefficient through the Soumpasis equation. The line inside the box is at the mean of the data and the box spans the minimum to the maximum.

S11: CryoTEM of FITC and TAMRA PA Alone

For consistency with diluent PA experiments, FITC PA and TAMRA PA were dissolved to 17.32 mM with 30 mM NaOH, which is the molarity of 2 wt% diluent PA. These PA solutions were then diluted to 8.66 mM (the molarity of 1 wt% diluent PA) with pure water, and thermally annealed (80°C 30 minutes, slow cool overnight). The samples were then imaged as described in Section **S4**, except they were not diluted 1:100 times before blotting. Due to the lower viscosity of these samples, it was possible to blot them at 1 wt%.

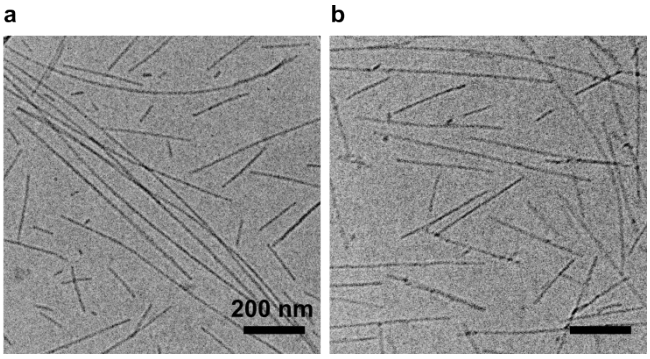

Figure S22. Cryogenic transmission electron micrographs (cryoTEM) of 8.66 mM annealed FITC PA **(a)** and 8.66 mM annealed TAMRA PA **(b)** Both samples were prepared without diluent PA.

S12: Mechanical Perturbation of Diluent PA Matrix

Two methods of mechanically perturbing the PA nanofibers were used: 1.) freeze-thawing and 2.) vortex mixing the PA solutions. Freeze-thawed samples were created by subjecting the annealed PA mixtures to ~30 seconds of submersion in liquid nitrogen, and allowing them to thaw at room temperature. Vortexed samples were created by subjecting the annealed PA mixtures to ~1 minute of vortexing.

Our laboratory previously characterized the effects of freeze-thawing on nanofibers in great detail, and showed that it breaks long nanofibers into noticeably shorter ones.[1] We presumed that vortexing would have a similar effect, and performed viscosity measurements, using the rheometer setup described in section **S8**. For these viscosity measurements, $V_3A_3E_3$ PA solutions were dissolved to 2 wt% with 30 mM NaOH, diluted to 1 wt% with pure water, and then thermally annealed (80°C 30 minutes, slow cool overnight). These samples did not contain fluorophore-labeled PA. Annealed samples were analyzed as they were, and vortexed samples were subject to 1 minute of vortexing.

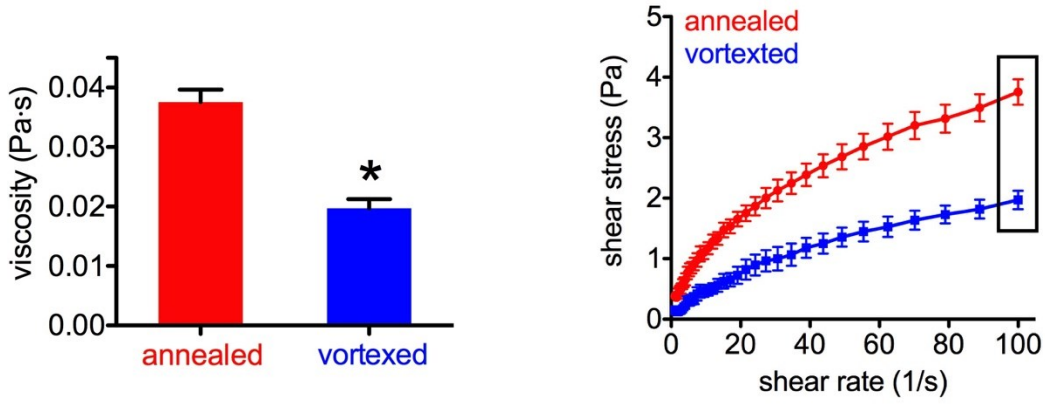

Figure S23: Left: Viscosity of annealed PA, and PA that was annealed and then vortexed. **Right:** Full flow curves of annealed PA and vortexed PA. The box indicates the data points used to calculate the viscosity reported in the graph on the left.

The effect of vortexing and freeze-thawing on annealed PA solutions was also observed by taking cross-polarized light micrographs. Annealed PA mixtures containing diluent, FITC, and TAMRA PA were prepared as described in section **S2**, using the same exact procedure as for FRET experiments. PA solutions (50 μL) were pipetted onto a glass cover slide, and observed between cross polarizers set to 90°. As expected, intact annealed PA solutions contain large aligned monodomains (Figure S24). After vortexing or freeze-thawing, the aligned monodomains do not disappear, but become "disrupted" and turn into smaller monodomains (Figure S24). This suggests that even as the nano-scale fibers break into shorter fragments, the hierarchical, micron-scale arrangement of the nanofibers do not disassemble.

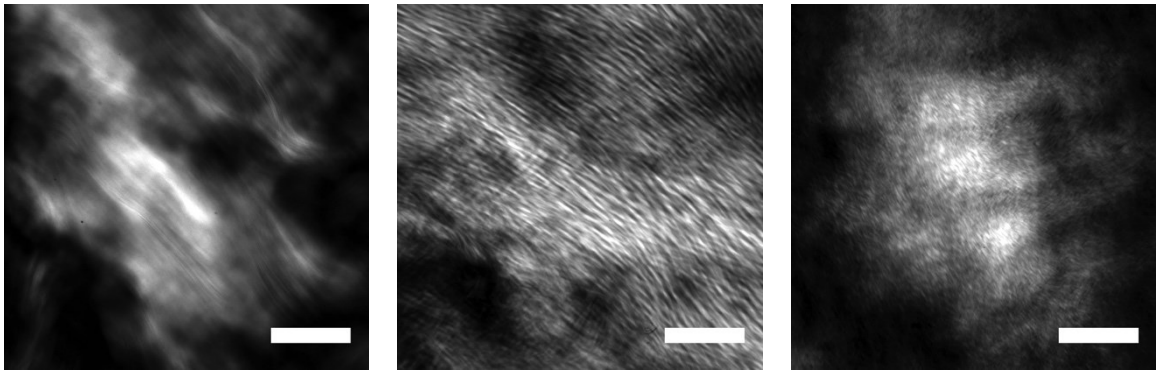

Figure S24: From left to right: Polarized light micrographs of annealed, annealed then vortexed, and annealed then freeze-thawed PA solutions. All scale bars are 200 μm.

Annealed diluent PA + FITC PA + TAMRA PA mixtures, at 1 wt% and containing no NaCl, were prepared as described in section **S2**. FRET spectra on these samples were collected as described in section **S2.** Rhodamine emission from direct excitation is also reported.

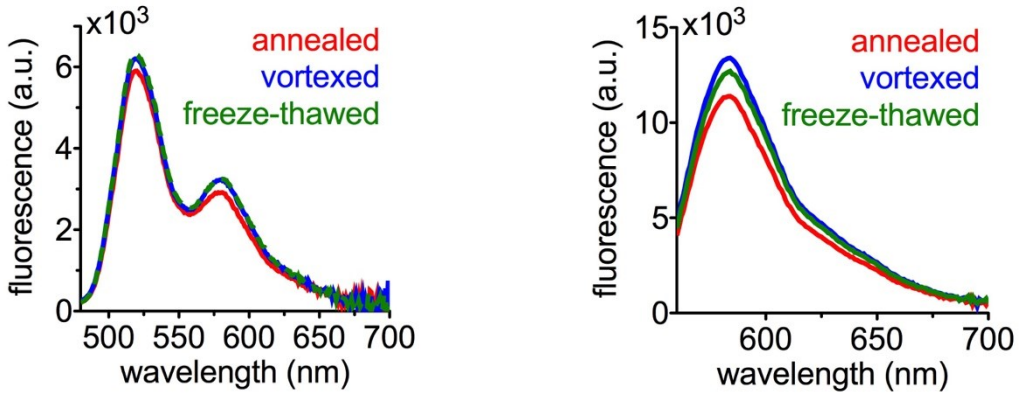

Figure S25. Left: FRET spectra annealed PA mixtures containing no salt, as is, after vortexing, and after freeze-thawing. Excitation: 450 nm. **Right:** TAMRA emission from direct excitation of the same samples shown on the left. Excitation: 530 nm.

S13: Introducing a Weak Hydrogen Bonding PA

We sought to disturb nanofiber cohesion in the diluent PA matrix by introducing a different PA molecule, which has a weaker propensity for hydrogen bonding due to its molecular design. This PA has the peptide sequence $A_3G_3E_3$ ("weak" PA, Figure **S25**), in contrast to $V_3A_3E_3$ PA ("strong" PA, Figure 1 in the main text). Both PAs have identical hydrophobic tails (C_{16}, palmitic acid) and charged headgroups (E_3, glutamic acids), but the peptide sequence A_3G_3 has much weaker propensity for β-sheet formation than V_3A_3. Our laboratory previously showed that weak PA self-assembles into less cohesive nanostructures than strong PA,[8, 9] which we confirmed in the current work with other techniques (Figure **S28**). We synthesized C_{16}-$A_3G_3E_3$ PA (weak diluent PA), and C_{16}-$A_3G_3E_3$K-FITC PA (weak FITC PA) molecules using the procedure described in section **S1**. The chemical structures and LC-MS analysis for purity are shown in Figures **S26-27**.

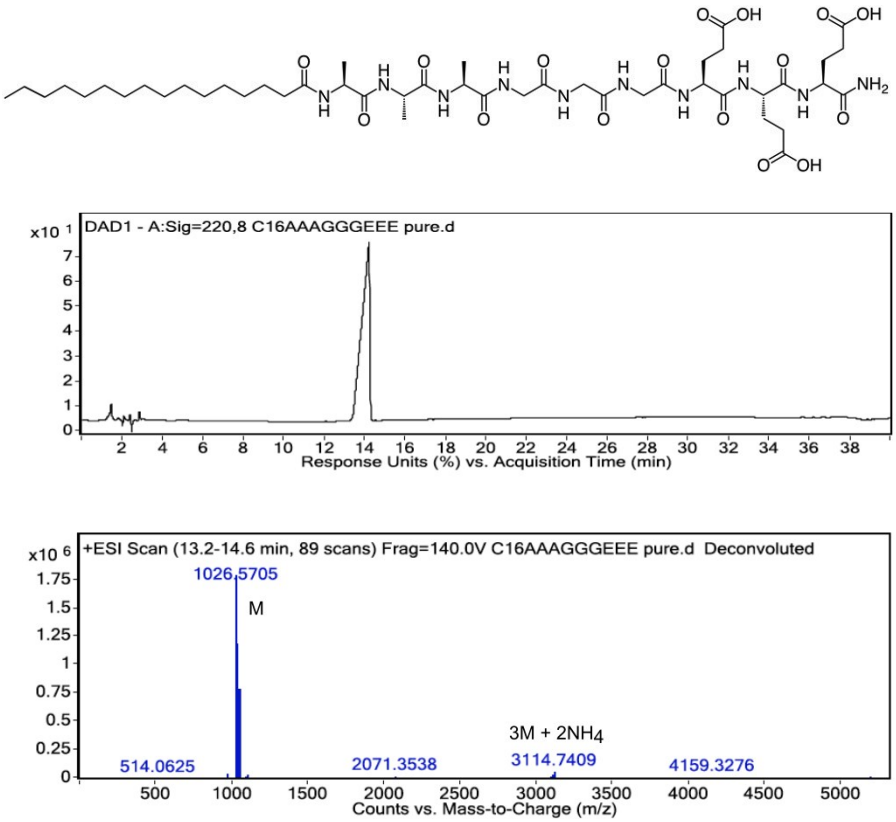

Figure S26. Chemical structure and LC-MS analysis of $A_3G_3E_3$ PA (weak PA).

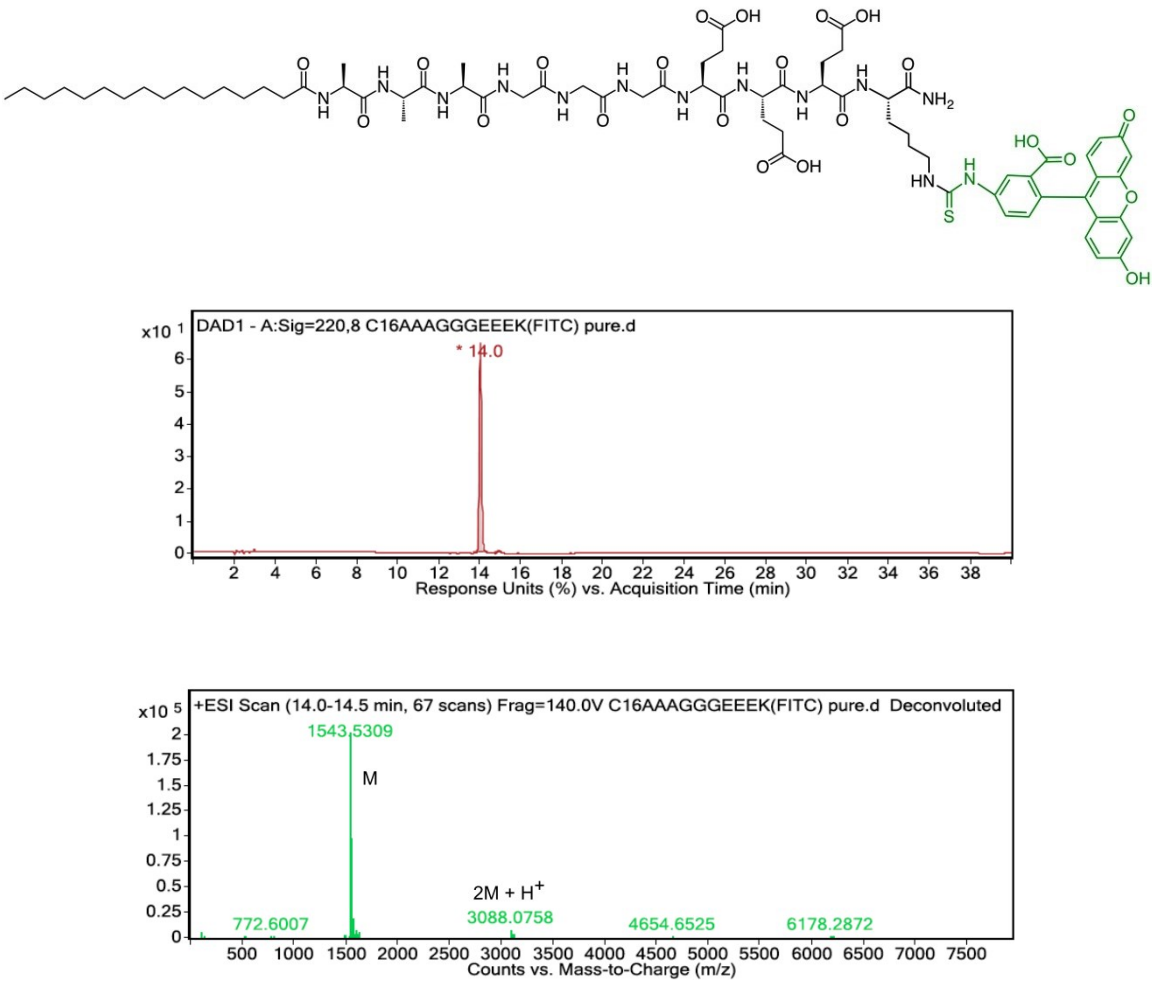

Figure S27. Chemical structure and LC-MS analysis of $A_3G_3E_3K$ -FITC PA (weak FITC PA).

Characterization of weak PA

Several techniques show the decreased propensity of **$A_3G_3E_3$ PA** for hydrogen bonding. The data also suggest that NaCl has no appreciable effect on the $A_3G_3E_3$ PA self-assembly. Weak diluent PA has the same negatively charged glutamic acids as strong $V_3A_3E_3$ PA, which should be susceptible to charge screening by NaCl. However, because

weak PA has a decreased propensity for hydrogen bonding, even when counterions screen the charges to allow closer association between molecules, the molecules will not hydrogen bond.

1.) Thioflavin T (ThT) assay: Weak diluent PA samples were prepared using the same procedure as for strong diluent PA, as described in section **S8,** except that instead of dissolving weak PA to 2 wt% initially, it was dissolved to 1.78 wt%. Thus, the weak PA solutions would be at the same molarity (8.66 mM) as a 2 wt% strong PA solution. The samples contain no fluorescent PA. The ThT assay was then performed as described in section **S8**, and the data is shown in Figure **S28a**. For comparison, the ThT signal of strong PA containing no salt is plotted. Unlike strong PA, weak PA does not enhance ThT signal, and the presence of salt does not change this.

2.) Circular Dichroism (CD): CD experiments were performed on freshly dissolved PA solutions, since the long nanofibers formed during annealing can scatter light and interfere with the signal. Strong and weak diluent PA samples containing no fluorescent PA first dissolved to 2 wt% and 1.78 wt%, respectively, so that the molarities would match (17.32 mM). These solutions were then diluted with equal volume of water or 300 mM NaCl, to get 8.66 mM PA. For analysis by CD, the final 8.66 mM PA solutions were diluted 1:20 in pure water and loaded into a 1 mm path length cuvette. A JASCO J-815 spectrophotometer was used to scan the samples from 190 – 250 nm, with a scan speed of 100 nm/minute. All data is the average of three scans, and is shown in Figure **S28b**. The strong PA shows a characteristic β-sheet signal, and appears to be enhanced upon addition of salt. Since anisotropic nanofibers can scatter circularly polarized light, it is not clear if this change is due to stronger hydrogen bonding or longer nanofibers that can result from stronger hydrogen bonding. Regardless, we note that the presence of salt somehow affects the self-assembly behavior of strong PA, an effect which is not observed with the weak PA. The weak PA shows a random coil-like signal both with and without added salt.

3.) Weak diluent PA and weak FITC PA were first separately dissolved to 1.78 wt% (1.78 wt% weak PA is the same molarity as 2 wt% strong PA). Next, 1%

(volume/volume) of weak FITC PA was added to the weak diluent PA solution. The samples were then diluted to 8.66 mM PA with either water or NaCl. PA samples (50 μL) were then loaded into a 96-well black plate with a clear bottom. The plate was read on a Cytation^{TM}3 (BioTek, Winooski, VT, USA), with excitation at 450 nm and emission spectra collected from 480 – 700 nm. The data in Figure **S28c** shows that, unlike the case with strong PA, the fluorescence is not quenched upon addition of salt.

These techniques all show the reduced propensity for weak PA to form β-sheet structures, and also that the presence of salt does not appear to affect the self-assembly behavior of weak PA.

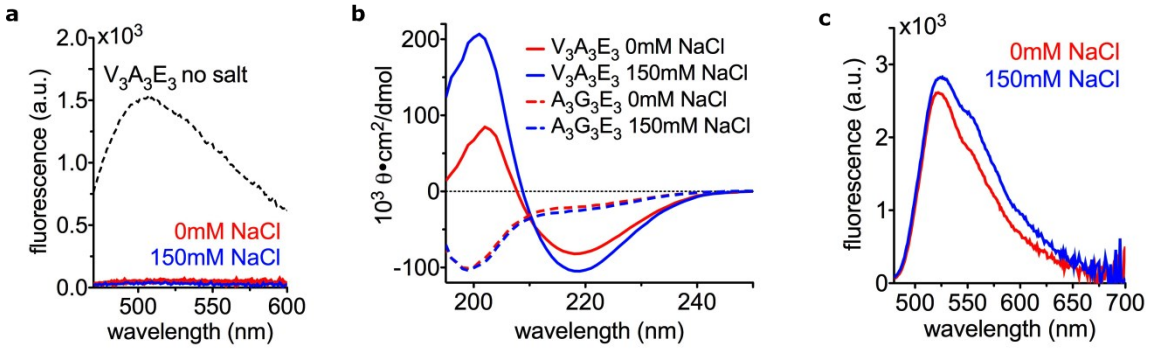

Figure S28. a) Thioflavin T (ThT) fluorescence in weak PA solutions, with and without NaCl as indicated. The ThT fluorescence in a strong PA solution with no salt is plotted for comparison (black dotted line). **b)** Circular dichroism spectra of strong and weak PA solutions, with and without NaCl as indicated. **c)** Fluorescence spectra of weak FITC PA, with and without salt as indicated.

FRET: Varying strong/weak PA Ratios in diluent matrix

Strong ($V_3A_3E_3$) PA was first dissolved to 1 wt% (8.66 mM) with 15 mM NaOH. To keep the molar concentration consistent, weak ($A_3G_3E_3$) PA was first dissolved to 0.89 wt%, which is 8.66 mM. This experiment contains no added NaCl. Fluorescent PAs ($V_3A_3E_3K$-TAMRA, $A_3G_3E_3K$-FITC) were dissolved to the same concentrations as their non-fluorescent counterparts. Before mixing strong and weak PA solutions, fluorescent PAs was added to their respective PA solutions. All mixtures contained the same amount

of fluorescent PA, regardless of the molar ratio of strong/weak unlabeled PA. This is illustrated below:

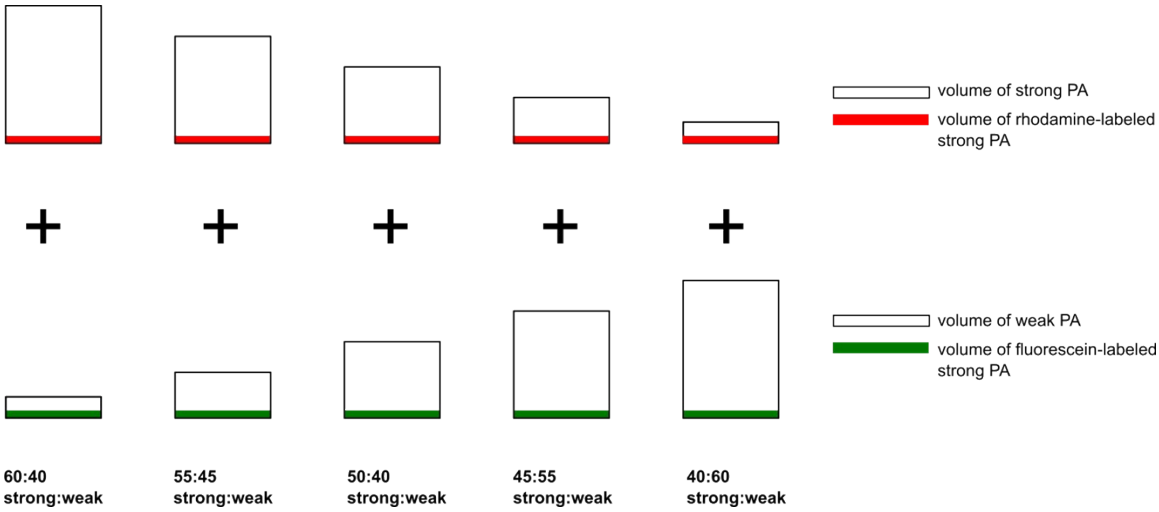

Figure S29: Schematic illustrating strong and weak PA solutions, containing the same molar concentration of PA. These solutions were mixed to give mixtures with different molar ratios of strong/weak diluent PA, but the same amount of fluorescent PA. Volumes are not drawn to scale, and are exaggerated for clarity.

The PA solutions (before mixing strong and weak solutions) for the 50:50 molar ratio sample had 1% volume/volume of fluorescent PA, and all other solutions received the same amount. Thus, the volume percentage of fluorescent PA to diluent PA varied from 0.0833 – 1.25% (60:40 vs. 40:60 molar ratio). Samples were thermally annealed for 80°C for 30 minutes, and slow-cooled overnight. FRET spectra were then collected as described in section **S2.** TAMRA emission from direct excitation at 530 nm is also shown.

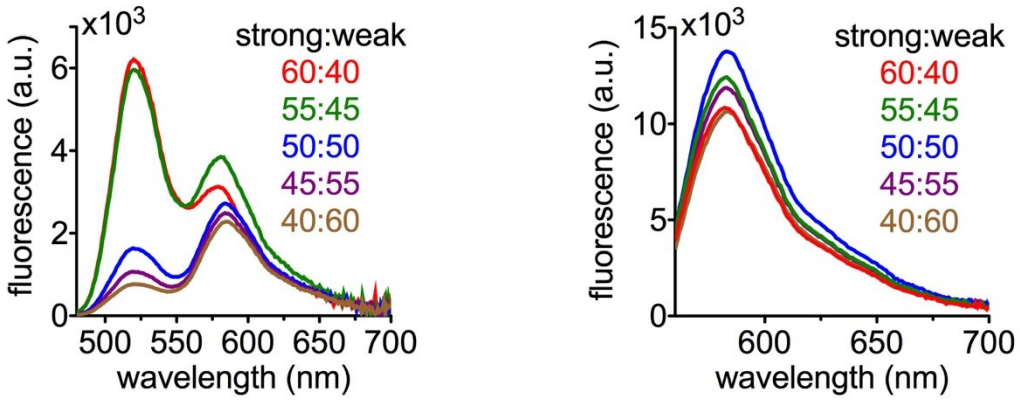

Figure S30. Left: FRET spectra of annealed PA mixtures containing weak and strong PA at indicated molar ratios. All samples contained no added NaCl. Excitation: 450 nm. **Right:** TAMRA emission from direct excitation of the same samples shown on the left. Excitation: 530 nm.

FRET: Adding NaCl to 60:40 strong/weak PA mixture

To allow for the addition of NaCl, strong PAs ($V_3A_3E_3$, $V_3A_3E_3$K-TAMRA) were first separately dissolved to 2 wt%, and weak PAs ($A_3G_3E_3$, $A_3G_3E_3$K-FITC) were first dissolved to 1.78 wt%, to keep the molarity of the diluent PA solutions constant. To keep the amount of fluorescent PA consistent with what it would be in a 50:50 mixture, strong diluent PA solutions received 0.833% (volume/volume) of its fluorescent analog ($V_3A_3E_3$K-TAMRA), while weak diluent PA solutions received 1.25% (volume/volume) of its fluorescent analog ($A_3G_3E_3$K-FITC). These solutions were then diluted with equal volume of either pure water or 300 mM NaCl, resulting in final concentrations of 1 wt% strong PA or 0.89 wt% weak PA (8.66 mM for both), and 0 or 150 mM NaCl. Strong and weak PA solutions, now containing their respective fluorescent PAs and appropriate NaCl amounts, were then mixed to achieve a 60:40 molar ratio of strong/weak PA. These mixtures were then thermally annealed at 80°C for 30 minutes and slow-cooled overnight. FRET spectra were then collected as described in section **S2.** TAMRA emission from direct excitation at 530 nm is also shown.

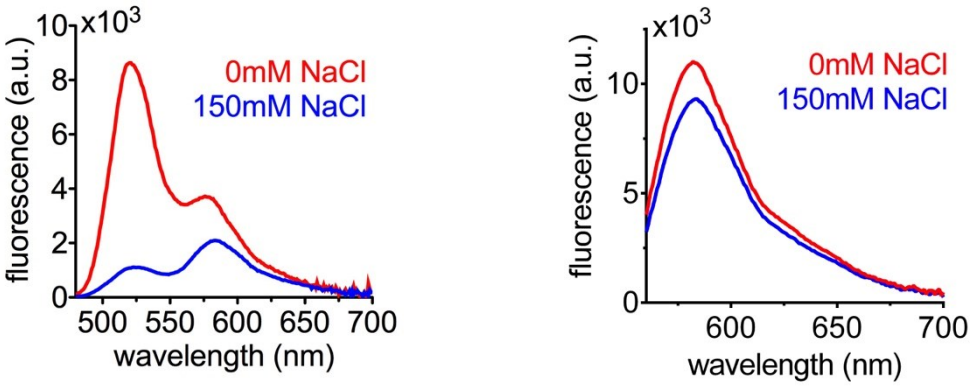

Figure S31: Left: FRET spectra of annealed PA mixtures containing a 60:40 molar ratio of strong/weak PA, with indicated concentration of NaCl. Excitation: 450 nm. **Right:** TAMRA emission from direct excitation of the same samples shown on the left. Excitation: 530 nm.

Annealed PA mixtures (same samples as in Figure **S30**, except no fluorescent PA was added) containing a 60:40 and 40:60 strong/weak diluent PA molar ratio, in 0 mM NaCl, were prepared as described above. An annealed PA mixture containing a 60:40 strong/weak PA molar ratio, in 150 mM NaCl, was also prepared as described above (same sample as in Figure **S31**, except no fluorescent PA was added). These samples were all imaged by cryoTEM using the procedure described in section **S4**. Despite the differences in FRET spectra when fluorescent PA is added (Figure **S30-31**), the self-assembled nanofibers in all samples appear similar, with no obvious morphological differences.

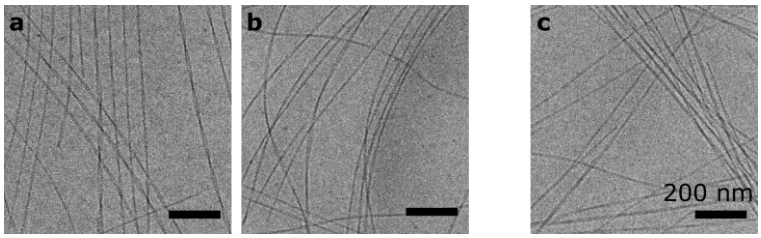

Figure S32. CryoTEM images of PA mixtures containing a strong/weak PA molar ratio of **a)** 60:40, in 0 mM NaCl, **b)** 40:60 in 0 mM NaCl, and **c)** 60:40 in 150 mM NaCl.

In the strong/weak PA systems described above, the "diluent PA matrix" can be thought of as the supramolecular nanostructures formed by a mixture of strong and weak diluent PA. The cryoTEM micrographs suggest that this matrix consists of long nanofibers (Figure **S32**), not unlike that formed by strong diluent PA (Figure 2f-h in the main text). The fluorescent PAs ($V_3A_3E_3K$-TAMRA, $A_3G_3E_3K$-FITC) can then interact with this supramolecular matrix. As shown in Figure **S29**, the fluorescent PA amounts do not change while the diluent PA amounts (strong/weak PA ratio) do, so the changes in FRET can be attributed to the diluent PA matrix.

References

1. Chen, C. H.; Palmer, L. C.; Stupp, S. I. *Nano Lett.* **2018,** 18, (11), 6832-6841.
2. Levine, H. *Protein Sci.* **1993,** 2, (3), 404-410.
3. Ortony, J. H.; Newcomb, C. J.; Matson, J. B.; Palmer, L. C.; Doan, P. E.; Hoffman, B. M.; Stupp, S. I. *Nat. Mater.* **2014,** 13, (8), 812-816.
4. Deka, C.; Lehnert, B.; Lehnert, N.; Jones, G.; Sklar, L.; Steinkamp, J. *Cytometry Part A* **1996,** 25, (3), 271-279.
5. Tantakitti, F.; Boekhoven, J.; Wang, X.; Kazantsev, R. V.; Yu, T.; Li, J.; Zhuang, E.; Zandi, R.; Ortony, J. H.; Newcomb, C. J.; Palmer, L. C.; Shekhawat, G. S.; Olvera de la Cruz, M.; Schatz, G. C.; Stupp, S. I. *Nat. Mater.* **2016,** 15, (4), 469-76.
6. Soumpasis, D. M. *Biophys. J.* **1983,** 41, (1), 95-97.
7. Motulsky, H. J.; Brown, R. E. *BMC Bioinformatics* **2006,** 7, (123).
8. Newcomb, C. J.; Sur, S.; Lee, S. S.; Yu, J. M.; Zhou, Y.; Snead, M. L.; Stupp, S. I. *Nano Lett.* **2016,** 16, (5), 3042-3050.
9. Newcomb, C. J.; Sur, S.; Ortony, J. H.; Lee, O.-S.; Matson, J. B.; Boekhoven, J.; Yu, J. M.; Schatz, G. C.; Stupp, S. I. *Nat. Commun.* **2014,** 5.